JAAS

PAPER

View Article Online
View Journal | View Issue

Cite this: J. Anal. At. Spectrom., 2018, 33, 1932

An optimized protocol for high precision measurement of Hg isotopic compositions in samples with low concentrations of Hg using MC-ICP-MS†

Hongyan Geng, [ab] Runsheng Yin[cd] and Xiangdong Li *[ad]

Multi-collector inductively coupled plasma mass spectrometry (MC-ICP-MS) enables the precise determination of mercury (Hg) isotopic compositions in different types of samples. However, isotopic measurements in samples with low Hg concentrations and small sample mass remain a challenge. In this study, we developed an optimized protocol for high precision Hg isotope determination using a modified cone arrangement (X skimmer cone + jet cone) with Neptune Plus MC-ICP-MS. Through modification of the HGX-200 continuous-flow cold-vapor generation system, and careful optimization of the instrument gas flow rates, we obtained steady and high signal sensitivity for Hg (^{202}Hg: 1.78 V per ng mL^{-1}). Our method allowed the precise determination of low Hg concentration in solutions (0.10 ng mL^{-1}), which is the lowest according to the literature. Only 0.70 ng Hg in samples was required according to our new analytical method, which enables the direct measurement of low Hg concentration in samples (down to 5 ng g^{-1}), after direct acid digestion treatment. Using our method, the Hg isotopic compositions of four igneous rock standard reference materials (BCR-2, BHVO-2, GSP-2, and GSR-2) were reported for the first time. The standard reference materials showed large variations of δ^{202}Hg (−1.24 to −2.47‰), indicating that mass dependent fractionation (MDF) of Hg isotopes occurred during magmatic processes.

Received 28th July 2018
Accepted 5th September 2018

DOI: 10.1039/c8ja00255j

rsc.li/jaas

1. Introduction

With the development of multi-collector inductively coupled plasma mass spectrometry (MC-ICP-MS), stable isotopes of Hg have been successfully used as tracers to understand the geochemical cycling of Hg in the environment.[1–3] Mercury has seven natural stable isotopes (^{196}Hg, ^{198}Hg, ^{199}Hg, ^{200}Hg, ^{201}Hg, ^{202}Hg and ^{204}Hg), which undergo both mass dependent fractionation (MDF, mostly reported as δ^{202}Hg) and mass independent fractionation (MIF, mainly reported as Δ^{199}Hg, Δ^{200}Hg, and Δ^{201}Hg) during various physical, chemical, and biological processes.[1,2] Natural samples from the Earth's reservoirs have shown large variations of >10‰ in both δ^{202}Hg and Δ^{199}Hg values, which are attributed to the isotope fractionation processes.[2] Combining the MDF and MIF signatures of Hg, Hg isotopes can provide multi-dimensional information to identify the sources and biogeochemical pathways of Hg in various sample media.

For Hg isotopic composition analysis, the commercial HGX-200 continuous-flow cold-vapor generation system (CETAC Technologies, USA) has been conventionally used for sample introduction into MC-ICP-MS.[4–6] This introduction approach consists of continuously reducing Hg in solutions using $SnCl_2$ and generating Hg(0) vapor, which gives a low matrix effect, and steady and continuous Hg signals. Such a technique requires substantial amounts of Hg, but tends to greatly improve the external precision of the measurements. For samples with high Hg concentrations (*i.e.*, ≥25 ng g^{-1}), the samples can be acid digested with perfect Hg recoveries (>90%), and diluted to appropriate Hg concentrations (0.5–5 ng mL^{-1}) and acid concentrations (<20%, v/v), and directly measured using MC-ICP-MS. The results showed small uncertainties of 0.10‰ (2SD) and 0.05‰ (2SD) for δ^{202}Hg and Δ^{199}Hg, respectively.[5–8] At least 5–10 mL of solution is normally required for Hg isotope analysis.[5–8]

For samples with low concentrations of Hg (<25 ng g^{-1}), such as igneous and metamorphic rocks, however, the isotopic composition determination is challenging using the conventional method. Even with 100% recovery, the dilution of acid concentrations to <20% would cause low Hg concentrations

[a]University Research Facility in Chemical and Environmental Analysis (UCEA), The Hong Kong Polytechnic University, Hung Hom, Kowloon, Hong Kong. E-mail: cexdli@polyu.edu.hk; Fax: +852 2334 6389; Tel: +852 2766 6041

[b]Shandong Provincial Key Laboratory of Depositional Mineralization and Sedimentary Minerals, College of Geological Sciences and Engineering, Shandong University of Science and Technology, Qingdao 266590, China

[c]State Key Laboratory of Ore Deposit Geochemistry, Institute of Geochemistry, Chinese Academy of Sciences, Guiyang 550002, China

[d]Department of Civil and Environmental Engineering, The Hong Kong Polytechnic University, Hung Hom, Kowloon, Hong Kong

† Electronic supplementary information (ESI) available. See DOI: 10.1039/c8ja00255j

(*i.e.*, <0.5 ng mL^{-1}), which makes Hg isotope analysis difficult. To solve this problem, gold trapping,[9] activated carbon trapping,[10] $KMnO_4 + H_2SO_4$ trapping[11–16] and chromatographic pre-concentration[17] were developed to pre-concentrate Hg to appropriate levels (≥0.5 ng mL^{-1} Hg). Although these pre-concentration techniques enable the isotopic analysis of samples with low Hg concentration, it is noteworthy that pre-concentration suffers from tedious procedures, which are not only time consuming and involve the use of chemicals, but also pose a risk of Hg isotope fractionation due to Hg loss (or contamination) in the processes. More importantly, for precious samples with limited availability, such as meteorite and aerosol samples, the measurement of Hg isotopic composition is not possible by acid digestion and pre-concentration methods due to the limited amount of Hg in samples.

An alternative way of measuring samples with low concentrations of Hg and those with limited availability is to directly improve the Hg sensitivity of the instrument. The uncertainty of the Hg isotope ratio decreases when the Hg signal intensity is increased, and therefore the improvement of Hg sensitivity will enable the precise measurement of low Hg concentration in solutions. The new generation Neptune Plus MC-ICP-MS (Thermo Electron Corp, Bremen, Germany), which has combined modified skimmer and sample cone geometries with an enhanced interface pumping configuration, has largely enhanced the ion sampling efficiency and overall signal sensitivity. It is worth noting that the Hg signal sensitivity of the instrument is also dependent on the types of introduction systems and the gas flow rates. In a recent study, the use of modified cones combined with an adapted cold-vapor generator resulted in higher Hg sensitivity than that of the traditional methods, which enabled the precise measurement of low Hg concentration in solutions (0.3 ng mL^{-1}).[18]

In the present study, we modified the continuous-flow cold-vapor generation system based on the HGX-200 system. Through careful optimization of the instrument gas flow rates, we achieved a much higher signal sensitivity of 1.78 V per ng mL^{-1} Hg for ^{202}Hg. With this signal sensitivity, high precision measurement of much lower Hg concentration in solutions (0.10 ng mL^{-1}) was achieved. Our method enabled the direct measurement of low Hg concentration in samples (as low as 5 ng g^{-1}), after direct acid digestion treatment. Using our developed method, the Hg isotope compositions of four igneous rock reference materials were measured and reported for the first time. In addition, how to optimize the Hg isotope signals has always been a conundrum because it has rarely been clearly described in pervious publications. Based on our experiments, visible correlations were obtained between the Hg signal intensity and the gas flow rates. The present study, therefore, deciphers this procedure by presenting a visualized correlation between the Hg signal intensity and the gas flow rates.

2. Experimental methods

2.1 Reagents

Hg (NIST SRM 3133) and Tl (NIST SRM 997) standard solutions were purchased from the National Institute of Standards and Technology (NIST, U.S. Department of Commerce). The UM-Almadén secondary Hg standard solution, produced by the University of Michigan, USA, was provided by Professor Dongxing Yuan from Xiamen University, China. Ultra-pure acids (HCl and HNO_3) were used to prepare the standard solutions and digest the samples. $SnCl_2$ (3%, w/w) was prepared in 10% (v/v) HCl. 18.2 MΩ cm water (ELGA LabWater) was used for the preparation of reagents and solutions.

2.2 Digestion of the standard reference materials

NIST SRM 2711a (Montana II Soil) and four igneous rock standard reference materials (SRMs), including BCR-2 (basalt), BHVO-2 (basalt), GSP-2 (granodiorite) and GSR-2 (andesite), were digested for Hg isotopic composition analysis. Briefly, approximately 0.4 g of each SRM was digested using 4 mL of aqua regia (HCl/HNO_3 = 3, v/v) in a water bath (95 °C) for 2 hours, following the method reported previously.[19–21] Acid blanks were prepared for each test. The Hg blanks for acids had concentrations <20 pg mL^{-1}. The relative standard deviation for sample duplicates was within 10% of the measured values.

2.3 Instrumental setting

Mercury isotope measurements were conducted on a Neptune Plus MC-ICP-MS housed at the University Research Facility in Chemical and Environmental Analysis (UCEA) in the Hong Kong Polytechnic University. The instrument was equipped with the HGX-200 system and an Aridus II Desolvating Nebulizer System (CETAC Technologies, USA) for Hg and Tl introduction, respectively. $SnCl_2$ was continuously pumped along with Hg(II) solutions and allowed to mix prior to introduction into the HGX-200 system, producing gaseous elemental Hg(0). In the chamber of HGX-200, the Hg(0) was mixed with the dry Tl aerosol generated by the Aridus II desolvating nebulizer before being introduced into the plasma (Fig. 1a). A computer-controlled Perimax Spetec peristaltic pump (Spetec GmbH, Germany) and a PFA-50 nebulizer were used for the uptake of Hg and Tl solutions, with the uptake rates of about 0.63 mL min^{-1} and 0.05 mL min^{-1}, respectively.

As shown in Fig. 1b(1), "additional gas 2", which is used for delivering Tl aerosols from the Aridus II desolvating nebulizer, was originally connected to the left side of HGX-200. The "sample gas", which is used for delivering Hg(0) vapor, was originally connected to the right side of HGX-200. We found that such a connection generated fluctuating Hg signals. The fluctuation of Hg signals may be explained by the fact that "additional gas 2" usually had much higher flow rates than the "sample gas" (Table 1). The higher flow rates of "additional gas 2" caused relatively higher pressure in the chamber, which tends to suppress the flow of "sample gas" through the chamber. In this circumstance, the "sample gas" accumulated and the pressure below the chamber increased. When the accumulated pressure surpassed the pressure in the chamber, the "sample gas" quickly broke through the chamber. Then the accumulation continued below the chamber until another "sample gas" broke through, which caused the fluctuating Hg signal. To solve this problem, the Teflon filter originally located

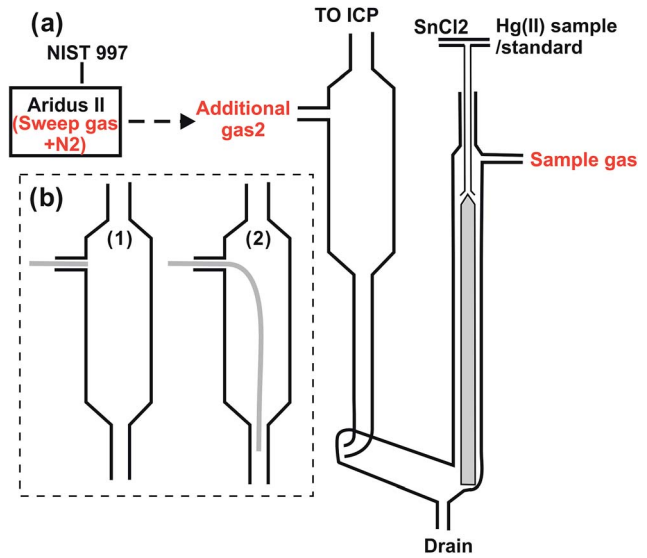

Fig. 1 (a) Sketch of the sample introduction system. (b(1)) The original setting of the tubing of "additional gas 2", which produces fluctuating Hg signals. (b(2)) The modified setting, where the tubing is extended below and gives stable Hg signals.

Table 1 Operating parameters for Hg isotope analysis

MC-ICP-MS	
Cool gas (Ar)	16.00 L min^{-1}
Auxiliary gas (Ar)	0.8 L min^{-1}
Sample gas (Ar)	0.181 L min^{-1}
Additional gas 2 (Ar)	1.7 L min^{-1}
X-Pos	−3.76 mm
Y-Pos	−1.76 mm
Z-Pos	−3.43 mm
RF power	1200 W
Extraction	−1610 V
Focus	−502 V
X-Defl	6.49 V
Y-Defl	−0.73 V
Shape	208 V
Rot quad 1	6.07 V
Source offset	1.00 V
Focus quad	10 V
Dispersion quad	0 V
Aridus II	
Nebulizer	PFA-50
Sweep gas (Ar)	3.31 L min^{-1}
Addition gas (N_2)	0 L min^{-1}

in the middle of the chamber was removed (note that many studies did not use a filter in their Hg introduction system), and the tubing of "additional gas 2" was extended below the chamber (Fig. 1b(2)). After these changes, "additional gas 2" mixed well with the "sample gas" before entering the chamber, and therefore stable Hg signals were obtained.

2.4 Mercury isotope determination

The NIST SRM 997 Tl standard ($^{205}Tl/^{203}Tl = 2.38714$) was used as an internal standard for simultaneous instrument mass bias correction of Hg. Nine Faraday cups L4, L3, L2, L1, C, H1, H2, H3 and H4 were used to monitor the ^{198}Hg, ^{199}Hg, ^{200}Hg, ^{201}Hg, ^{202}Hg, ^{203}Tl, ^{204}Hg, ^{205}Tl and ^{206}Pb isotopes, respectively. A nickel X skimmer cone combined with a jet cone was employed in the tests. Hg and Tl concentrations in solutions were monitored using ^{202}Hg and ^{205}Tl signal intensities. The signal intensity of ^{202}Hg was approximately 10 mV for 10% (v/v) acid blanks. Isobaric interference of ^{204}Pb on ^{204}Hg was evaluated by measuring the signal intensity of ^{206}Pb, which was $<10^{-4}$ V during the analytical session, suggesting limited interference of ^{204}Pb on ^{204}Hg.

The gains of the amplifier associated with each Faraday collector were calibrated for efficiency on a daily basis. Instrumental parameters (*e.g.*, gas flow rate, torch settings, and the lens system) were tuned to guarantee steady signals, high intensities and good peak shapes. Data were acquired using 2.097 seconds per cycle, similar to previous studies.[5,18] An ASX-112FR Flowing Rinse Micro Autosampler (CETAC Technologies) was employed for every test. Between samples, the autosampler was rinsed using 3% (v/v) HNO_3 for 3.5 minutes until Hg signal intensity returned to the background level. Following the protocol of Blum and Bergquist,[6] the sample–standard bracketing (SSB) approach was used to compare the relative permil (‰) deviation (using the δ notation) of all our measurements to that of NIST SRM 3133, according to eqn (1):

$$\delta^{xxx}\mathrm{Hg}\ (‰) = [(^{xxx}\mathrm{Hg}/^{198}\mathrm{Hg}_{\mathrm{sample}})/(^{xxx}\mathrm{Hg}/^{198}\mathrm{Hg}_{\mathrm{NIST3133}}) - 1] \times 1000 \quad (1)$$

where the *xxx* value is 199, 200, 201, 202 and 204 amu. Hg-MIF is reported in Δ notation ($\Delta^{xxx}Hg$, deviation from mass dependency in units of permil, ‰) and is the difference between the measured $\Delta^{xxx}Hg$ and the theoretically predicted $\Delta^{xxx}Hg$ value following eqn (2)–(5):

$$\Delta^{199}\mathrm{Hg} \approx \delta^{199}\mathrm{Hg} - \delta^{202}\mathrm{Hg} \times 0.2520 \quad (2)$$

$$\Delta^{200}\mathrm{Hg} \approx \delta^{200}\mathrm{Hg} - \delta^{202}\mathrm{Hg} \times 0.5024 \quad (3)$$

$$\Delta^{201}\mathrm{Hg} \approx \delta^{201}\mathrm{Hg} - \delta^{202}\mathrm{Hg} \times 0.7520 \quad (4)$$

$$\Delta^{204}\mathrm{Hg} \approx \delta^{204}\mathrm{Hg} - \delta^{202}\mathrm{Hg} \times 1.4930 \quad (5)$$

3. Results and discussion

3.1 Effects of "additional gas 2" and "sample gas" flow rates on signal intensities

Four gas flows, *i.e.*, Ar sweep gas and N_2 addition gas of the Aridus II Desolvating Nebulizer System, and "additional gas 2" and "sample gas" of HGX-200, were used in our method (Fig. 1a). The flow rates of Ar sweep gas and N_2 addition gas were controlled using on-board rotameters, and the flow rates of "additional gas 2" and "sample gas" were controlled using a computer. NIST SRM 3133 (1 ng mL^{-1} Hg in 10% HCl) and NIST SRM 997 (50 ng mL^{-1} Tl in 3% HNO_3) standard solutions were employed in the test. Based on the initial flow rates of 1.0 L min^{-1} and 0.3 L min^{-1} for "additional gas 2" and "sample

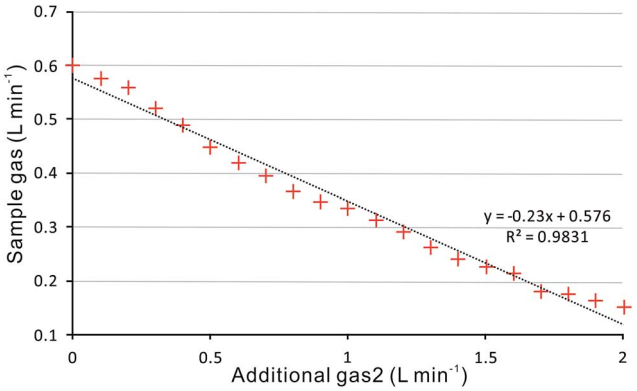

Fig. 2 Relationship between the flow rates of "additional gas 2" and "sample gas".

gas", respectively, the torch position, source lens, zoom optics of MC-ICP-MS, and the Ar sweep gas and N_2 addition gas of the Aridus II Desolvating Nebulizer System were tuned for a maximum ^{202}Hg signal intensity. These optimal parameters, as summarized in Table 1, remained unchanged in the later tests.

To test the effects of "additional gas 2" and "sample gas" flow rates on signal intensities, the flow rate of "additional gas 2" was first set to 0 L min^{-1}, and that of "sample gas" was adjusted to achieve the maximum ^{202}Hg signal intensity, and the signal intensities of Hg and Tl were recorded. Then the flow rate of "additional gas 2" was increased to 0.1 L min^{-1}, and that of the "sample gas" was tuned to reach the maximum ^{202}Hg signal intensity again, and the Hg and Tl signal intensities were also recorded. The above processes were repeated with an increment of 0.1 L min^{-1} for "additional gas 2" until the flow rate reached the maximum (2 L min^{-1}), which enabled us to build curves (Fig. 2 and 3) to fully understand the effects of "additional gas 2" and "sample gas" flow rates on signal intensities, as shown in Table S1.†

A negatively linear correlation between "additional gas 2" and "sample gas" flow rates was observed (Fig. 2). Since "additional gas 2" usually had much higher flow rates than the "sample gas" (Table 1), high flow rates of "additional gas 2" and low flow rates of "sample gas" were required to achieve the highest signal intensity of Hg in the analysis. More interestingly, a positively linear correlation between the flow rate of "additional gas 2" and ^{202}Hg signal intensity (Fig. 3a), and a negatively linear correlation between the flow rate of "sample gas" and ^{202}Hg signal intensity (Fig. 3b) were observed. These correlations may be explained by the fact that high flow rates of "sample gas", which delivers Hg(0) vapor, tend to dilute Hg signals. High flow rates of "additional gas 2" would also dilute the Hg signal, however, "additional gas 2" carries Tl aerosols. We hypothesize that the Tl aerosols may adsorb a substantial amount of Hg(0) vapor, which helps to improve the Hg signal intensity. Our hypothesis is supported by the fact that the Hg signal intensity dropped rapidly when the Aridus II Desolvating Nebulizer System introduced air instead of Tl aerosols.

The change of the flow rates of "additional gas 2" and "sample gas" also affected Tl signal intensities. As shown in Fig. 3c, the intensity of the ^{205}Tl signal was close to zero when the flow rates of "additional gas 2" ranged from 0 to 0.4 L min^{-1}, indicating that limited Tl was delivered with low "additional gas 2" flow rates. When the flow rate of "additional gas 2" increased to >0.4 L min^{-1}, ^{205}Tl signals emerged, and their intensities increased until the flow rate of "additional gas 2" reached 1.0 L min^{-1} (Fig. 3c). This indicated that the increase of "additional gas 2" flow rate in a certain range (0.4–1.0 L min^{-1}) was able to increase the delivery of Tl. When the flow rate of "additional gas 2" increased further (1.0–2.0 L min^{-1}), ^{205}Tl signal intensities decreased gradually (Fig. 3c). This indicated that high flow rates of "additional gas 2" (1.0–2.0 L min^{-1}) tended to dilute the Tl signal intensities. The change of flow rates of "sample gas" resulted in a curve that is a mirror image to that obtained for "additional gas 2" (Fig. 3d), which can be explained by the

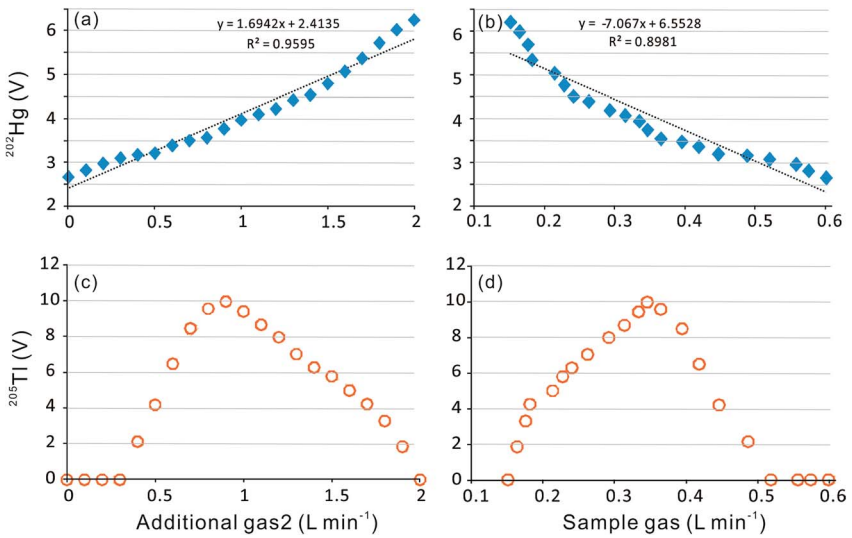

Fig. 3 Gas flow rates *vs.* ^{202}Hg intensity and ^{205}Tl intensity.

inverse correlation between the two gases (Fig. 2). ^{202}Hg showed a consistently linear increase (Fig. 3a) while ^{205}Tl showed a parabolic curve as the "additional gas 2" flow rates increased (Fig. 3c). It can be seen that with the "additional gas 2" flow rate of 1.7 L min^{-1}, ^{202}Hg and ^{205}Tl had comparable signal intensities. Therefore, 1.7 L min^{-1} was chosen as the optimized "additional gas 2" flow rate for our method. With this flow rate, the ^{202}Hg signal sensitivity of 1.78 V per ng mL^{-1} can be reached when tuning the "sample gas" flow rate to 0.181 L min^{-1}. The high Hg sensitivity (^{202}Hg: 1.78 V per ng mL^{-1}) at a low "sample gas" flow rate may be explained by the removal of the Teflon filter from our introduction system. Mercury has a relatively high ionization potential. Decreasing the "sample gas" flow rate would permit greater time in plasma for ionization. The removal of the Teflon filter from our introduction system and using "additional gas 2" created a diluted gas, which could decrease the high rate of gas flow to the plasma, and therefore permitted more efficient ionization of Hg.

3.2 Mercury isotope determination in solutions with low Hg concentration

Based on the optimized instrumental conditions (Table 1) and gas flow rates ("additional gas 2" = 1.7 L min^{-1}; "sample gas" = 0.181 L min^{-1}), UM-Almadén secondary Hg standard solution was diluted to 1.0, 0.7, 0.5, 0.4, 0.3, 0.2, and 0.1 ng mL^{-1} in 10% HCl (v/v) for Hg isotope analysis, using the SSB approach. The bracketed NIST SRM 3133 Hg solutions were diluted to have the same Hg concentrations and acid matrices as the UM-Almadén standard. For a certain Hg concentration, replicate measurements (n = 7) were performed. Georg and Newman demonstrated that the use of the X skimmer cone with the Neptune Plus MC-ICP-MS may cause the formation of Hg hydrides, which results in an artificial change in ^{205}Tl/^{203}Tl and mass bias during Hg isotope analysis.[7] However, a recent study by Yin *et al.*[18] proved that Hg hydride formation is less important when the Hg isotope measurements are conducted with high Tl concentrations (20–50 ng mL^{-1} Tl). In our study, the NIST SRM 997 (50 ng mL^{-1} Tl in 3% HNO_3) standard solution was used throughout the analysis.

For both UM-Almadén and NIST SRM 3133 solutions, Hg isotope ratios (*i.e.* ^{199}Hg/^{198}Hg, ^{200}Hg/^{198}Hg, ^{201}Hg/^{198}Hg, ^{202}Hg/^{198}Hg) increased with the increase of Hg concentrations (Fig. S1†), and the uncertainties of Hg isotope ratios increased with the decrease of Hg concentrations (Fig. 4). Similar patterns have been observed in a previous study.[18] As shown in Table 2 and Fig. 4, when transformed to δ and Δ values, UM-Almadén solutions at concentrations of 0.3, 0.4, 0.5, 0.7 and 1.0 ng mL^{-1} showed consistent Hg isotopic compositions with previous results,[6] indicating no anomalous mass bias. However, the UM-Almadén solution at a concentration of 0.1 ng mL^{-1} gave more scattered Hg isotopic compositions than previous results, and the UM-Almadén solution at a concentration of 0.2 ng mL^{-1} showed consistent Hg isotopic compositions but with larger standard deviations. It is noteworthy that the above tests were all performed using 3 blocks, 60 cycles per block and 2.097 seconds per cycle. Since each block gave stable and consistent isotopic compositions, we hypothesized that the detection limit can be pushed even lower, by increasing the sample uptake rate and decreasing the integration time. Our results showed that the Hg signal intensities can be nearly doubled by increasing the sample uptake rate from 0.63 to 1.26 mL min^{-1}. Only one block (60 cycles, 2.097 seconds per cycle) was used to test the isotopic composition of 0.1 and 0.2 ng mL^{-1} Hg solutions, with the sample uptake rate of 1.26 mL min^{-1} and 60 seconds of sample introduction time to guarantee stable Hg signal intensities, together with the simultaneous introduction of 50 ng mL^{-1} Tl. As shown in Table 2, 0.1 and 0.2 ng mL^{-1} Hg solutions then gave comparable results with previous studies.[6] An additional quality control measure was used for the isotope analysis of NIST SRM 2711a, which was diluted to 0.1 ng mL^{-1}

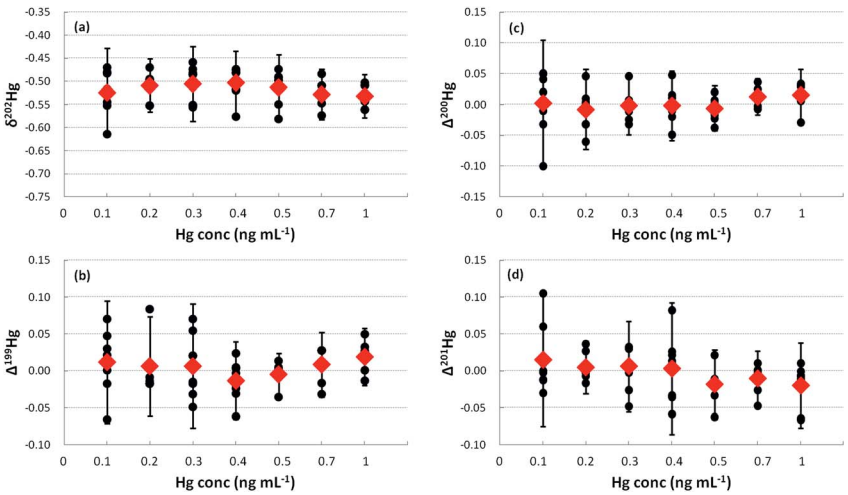

Fig. 4 Hg isotopic composition of UM-Almadén with different Hg concentrations. The tests for 0.1 and 0.2 ng mL^{-1} solutions were performed with the sample uptake rate of 1.26 mL min^{-1}, and using 1 block, 60 cycles per block and 2.097 seconds per cycle. The tests for other solutions were performed with the sample uptake rate of 0.63 mL min^{-1}, and using 3 blocks, 60 cycles per block and 2.097 seconds per cycle. The red diamond shows the average of the eight analyses for each concentration and the bar represents the error of the replicate analyses.

Table 2 Hg isotope composition of UM-Almadén. The tests for 0.1 and 0.2 ng mL^{-1} solutions were performed with the sample uptake rate of 1.26 mL min^{-1}, and using 1 block, 60 cycles per block and 2.097 seconds per cycle. The tests for other solutions were performed with the sample uptake rate of 0.63 mL min^{-1}, and using 3 blocks, 60 cycles per block and 2.097 seconds per cycle

Hg concentration (ng mL^{-1})	δ^{199}Hg (‰)	δ^{200}Hg (‰)	δ^{201}Hg (‰)	δ^{202}Hg (‰)	Δ^{199}Hg (‰)	Δ^{200}Hg (‰)	Δ^{201}Hg (‰)
0.1	−0.20	−0.37	−0.42	−0.54	−0.07	−0.10	−0.01
	−0.16	−0.31	−0.42	−0.55	−0.02	−0.03	0.00
	−0.10	−0.19	−0.26	−0.48	0.02	0.05	0.11
	−0.13	−0.22	−0.33	−0.52	0.00	0.04	0.06
	−0.05	−0.23	−0.39	−0.47	0.07	0.00	−0.03
	−0.11	−0.25	−0.35	−0.48	0.01	−0.01	0.01
	−0.11	−0.25	−0.40	−0.53	0.03	0.02	0.00
	−0.11	−0.26	−0.47	−0.61	0.05	0.05	−0.01
Average	−0.12	−0.26	−0.38	−0.52	0.01	0.00	0.01
SD	0.04	0.06	0.07	0.05	0.04	0.05	0.05
0.2	−0.10	−0.24	−0.33	−0.50	0.00	0.00	0.00
	−0.11	−0.25	−0.39	−0.50	0.01	0.00	−0.02
	−0.13	−0.19	−0.33	−0.47	−0.01	0.05	0.03
	−0.14	−0.31	−0.38	−0.49	−0.01	−0.06	−0.01
	−0.12	−0.25	−0.38	−0.51	0.01	0.01	0.00
	−0.16	−0.31	−0.42	−0.55	−0.02	−0.03	0.00
	−0.04	−0.25	−0.34	−0.50	0.08	0.00	0.04
	−0.16	−0.31	−0.42	−0.55	−0.02	−0.03	0.00
Average	−0.12	−0.26	−0.37	−0.51	0.01	−0.01	0.00
SD	0.04	0.04	0.04	0.03	0.03	0.03	0.02
0.3	−0.11	−0.27	−0.49	−0.46	−0.03	−0.02	0.03
	−0.12	−0.30	−0.45	−0.48	0.02	0.01	0.03
	−0.10	−0.24	−0.33	−0.49	0.02	0.01	0.03
	−0.13	−0.24	−0.35	−0.47	−0.01	0.00	0.00
	−0.16	−0.31	−0.42	−0.55	−0.02	−0.03	0.00
	−0.07	−0.23	−0.46	−0.55	0.07	0.05	−0.05
	−0.09	−0.28	−0.39	−0.56	0.05	−0.01	0.03
	−0.17	−0.25	−0.39	−0.48	−0.05	−0.01	−0.03
Average	−0.12	−0.26	−0.41	−0.51	0.01	0.00	0.01
SD	0.03	0.03	0.05	0.04	0.04	0.02	0.03
0.4	−0.10	−0.19	−0.28	−0.48	0.02	0.05	0.08
	−0.14	−0.26	−0.34	−0.48	−0.02	−0.02	0.02
	−0.15	−0.29	−0.35	−0.47	−0.03	−0.05	0.01
	−0.12	−0.23	−0.33	−0.48	0.00	0.01	0.03
	−0.14	−0.30	−0.42	−0.58	0.00	−0.01	0.01
	−0.19	−0.27	−0.43	−0.52	−0.06	0.00	−0.04
	−0.12	−0.24	−0.41	−0.50	0.00	0.02	−0.03
	−0.15	−0.26	−0.45	−0.52	−0.02	0.00	−0.06
Average	−0.14	−0.25	−0.38	−0.50	−0.01	0.00	0.00
SD	0.03	0.03	0.06	0.03	0.03	0.03	0.04
0.5	−0.14	−0.25	−0.40	−0.52	−0.01	0.01	−0.01
	−0.13	−0.25	−0.40	−0.50	−0.01	0.00	−0.02
	−0.14	−0.26	−0.42	−0.55	0.00	0.02	−0.01
	−0.13	−0.29	−0.45	−0.58	0.01	0.00	−0.01
	−0.13	−0.25	−0.41	−0.50	−0.01	0.00	−0.03
	−0.12	−0.26	−0.43	−0.49	0.01	−0.02	−0.06
	−0.15	−0.28	−0.37	−0.47	−0.04	−0.04	−0.02
	−0.13	−0.27	−0.35	−0.49	0.00	−0.02	0.02
Average	−0.13	−0.26	−0.40	−0.51	0.00	−0.01	−0.02
SD	0.01	0.02	0.03	0.04	0.01	0.02	0.02
0.7	−0.12	−0.25	−0.38	−0.51	0.01	0.01	0.00
	−0.11	−0.25	−0.40	−0.53	0.03	0.02	0.00
	−0.15	−0.28	−0.46	−0.55	−0.02	0.00	−0.05
	−0.18	−0.26	−0.44	−0.57	−0.03	0.02	−0.01
	−0.11	−0.25	−0.35	−0.48	0.01	−0.01	0.01
	−0.11	−0.23	−0.43	−0.54	0.03	0.04	−0.03
	−0.12	−0.25	−0.38	−0.51	0.01	0.01	0.00

Table 2 (*Contd.*)

Hg concentration (ng mL^{-1})	δ^{199}Hg (‰)	δ^{200}Hg (‰)	δ^{201}Hg (‰)	δ^{202}Hg (‰)	Δ^{199}Hg (‰)	Δ^{200}Hg (‰)	Δ^{201}Hg (‰)
	−0.11	−0.25	−0.40	−0.53	0.03	0.02	0.00
Average	−0.12	−0.25	−0.41	−0.53	0.01	0.01	−0.01
SD	0.03	0.01	0.03	0.03	0.02	0.01	0.02
1	−0.12	−0.28	−0.43	−0.56	0.02	0.01	−0.01
	−0.11	−0.25	−0.41	−0.56	0.03	0.03	0.01
	−0.12	−0.24	−0.40	−0.53	0.02	0.03	0.00
	−0.11	−0.24	−0.42	−0.54	0.03	0.03	−0.01
	−0.14	−0.28	−0.45	−0.51	−0.01	−0.03	−0.06
	−0.14	−0.24	−0.41	−0.54	0.00	0.03	−0.01
	−0.11	−0.25	−0.39	−0.50	0.02	0.01	−0.01
	−0.08	−0.24	−0.45	−0.51	0.05	0.02	−0.07
Average	−0.11	−0.25	−0.42	−0.53	0.02	0.02	−0.02
SD	0.02	0.02	0.02	0.02	0.02	0.02	0.03

Hg. As shown in Table 3, the results obtained during the multiple measurement sessions were in good agreement with previously published results.[22,23] Based on this, the detection limit of our current system can be confidently set at 0.10 ng mL^{-1}, which, to our knowledge, is the ultimate low value in the available publications.

The 0.3, 0.4, 0.5, 0.7 and 1.0 ng mL^{-1} tests were performed using 3 blocks, 60 cycles per block, and 2.097 seconds per cycle, with a total integration time of 380 seconds, plus 90 seconds of sample introduction to guarantee stable Hg signal intensities. The sample uptake was about 0.63 mL min^{-1}, in other words, at least 5.0 mL solution was required to accomplish each test. Similarly, for the 0.1 and 0.2 ng mL^{-1} tests, 4.0 mL solution was required. Since the sample probe of the autosampler cannot reach the very bottom of the tube, 7 mL of solution is required. In fact, the volume of our autosampler tube is 7 mL.

Considering that 7.0 mL of solution is necessary for our method, to obtain confident Hg isotope data, at least 0.7 ng Hg (0.10 ng mL^{-1} × 7.0 mL) is required. This is much lower than that used in previous studies, where at least 3–20 ng of Hg was used.[18] Considering that the acid concentration within each sample should be below 20%, for 7.0 mL diluted solution, the acid should be no more than 1.4 mL, which corresponds to the maximum of 0.14 g of sample used for digestion. In other words, our method can allow the direct measurement of Hg isotopic composition of samples with low Hg concentration (5 ng g^{-1} = 0.7 ng/0.14 g), using the acid digestion approach. Combined with the available pre-concentration methods,[10–17] the required amount of samples and chemicals may be further reduced. For example, for the analysis of samples with very low Hg concentration (<5 ng g^{-1}), the samples need to be pre-concentrated to achieve 0.70 ng Hg. This is extremely helpful for the measurement of precious samples (*e.g.*, meteorites and aerosol samples) with both low sample amounts and low Hg concentrations.

3.3 Igneous rock reference materials

Igneous rocks are one of the natural materials with low concentrations of Hg.[24] Four igneous rock SRMs, named BCR-2 (basalt), BHVO-2 (basalt), GSP-2 (granodiorite) and GSR-2 (andesite), were digested and tested for Hg isotopic compositions. The Hg concentration of the SRMs ranged from 6.0 to 22.2 ng g^{-1}, according to the ^{202}Hg signal intensities (Table 4). The Hg concentrations of the SRMs are within the range of previous results.[25] The SRMs were analyzed repeatedly over separate analytical sessions on different days, with Hg concentration in the digests of 0.12 to 0.44 ng mL^{-1} (Table 4). For solutions with Hg > 0.20 ng mL^{-1}, the isotopic compositions were measured using 3 blocks, 60 cycles per block, and

Table 3 Hg isotope composition of 0.1 ng mL^{-1} SRM NIST 2711a (Montana II Soil). The tests were performed with the sample uptake rate of 1.26 mL min^{-1}, and using 1 block, 60 cycles per block and 2.097 seconds per cycle

	δ^{199}Hg (‰)	δ^{200}Hg (‰)	δ^{201}Hg (‰)	δ^{202}Hg (‰)	Δ^{199}Hg (‰)	Δ^{200}Hg (‰)	Δ^{201}Hg (‰)
	−0.22	−0.03	−0.25	−0.09	−0.19	0.01	−0.18
	−0.23	−0.07	−0.26	−0.08	−0.21	−0.03	−0.20
	−0.24	−0.10	−0.26	−0.11	−0.21	−0.04	−0.17
	−0.22	−0.06	−0.26	−0.08	−0.20	−0.02	−0.20
	−0.28	−0.08	−0.26	−0.12	−0.25	−0.02	−0.17
	−0.23	−0.06	−0.26	−0.14	−0.19	0.01	−0.15
	−0.28	−0.08	−0.27	−0.07	−0.26	−0.04	−0.22
	−0.23	−0.04	−0.22	−0.07	−0.21	0.00	−0.17
Average	−0.24	−0.07	−0.25	−0.10	−0.22	−0.02	−0.18
SD	0.02	0.02	0.01	0.03	0.02	0.02	0.02

Table 4 Hg isotope compositions of the igneous rock SRMs

SRM	N	Hg (ng g^{-1})	Hg (ng mL^{-1})	δ^{199}Hg (‰)	SD (‰)	δ^{200}Hg (‰)	SD (‰)	δ^{201}Hg (‰)	SD (‰)	δ^{202}Hg (‰)	SD (‰)	Δ^{199}Hg (‰)	SD (‰)	Δ^{200}Hg (‰)	SD (‰)	Δ^{201}Hg (‰)	SD (‰)
BCR-2	5	6.8	0.14	−0.52	0.07	−1.04	0.04	−1.56	0.04	−2.08	0.04	0.00	0.07	0.01	0.04	0.00	0.07
BHVO-2	5	6.0	0.12	−0.65	0.05	−1.24	0.06	−1.84	0.04	−2.44	0.05	−0.03	0.04	−0.01	0.06	0.00	0.03
GSP-2	5	22.2	0.44	−0.29	0.08	−0.59	0.12	−0.88	0.11	−1.20	0.11	0.01	0.07	0.02	0.07	0.02	0.06
GSR-2	5	11.5	0.23	−0.26	0.06	−0.69	0.12	−1.09	0.19	−1.47	0.13	0.11	0.03	0.05	0.07	0.02	0.12

2.097 seconds per cycle, with the sample uptake rate of 0.63 min^{-1}. For solutions with Hg concentration ≤0.20 ng mL^{-1}, the isotopic compositions were measured using 1 block, 60 cycles per block, and 2.097 seconds per cycle, with the sample uptake rate of 1.26 min^{-1}. UM-Almaden was analyzed right after the analysis of each SRM. The Hg concentrations and acid matrices of NIST SRM 3133 were matched to the bracketed samples.

As shown in Table 4, the long-term reproducibility of the SRMs was comparable to that of the UM-Almadén secondary solution. The SRMs showed large variations in δ^{202}Hg (−1.24 to −2.47‰) but little variation in Δ^{199}Hg (0.01 to 0.11‰), indicating that MDF rather than MIF of Hg isotopes occurred during magmatic processes. Our results for the granodiorite (GSP-2) and andesite (GSR-2) SRMs were similar to those reported for volcanic rocks of the Clear Lake Volcanic Field, USA (δ^{202}Hg: −1.20‰ to −0.25‰; Δ^{199}Hg ∼ 0),[25] but the basalt SRMs (BCR-2, BHVO-2) showed much lower δ^{202}Hg values, indicating that the isotopic compositions in igneous rocks are largely variable, with lower δ^{202}Hg in mafic rocks, and higher δ^{202}Hg in felsic rocks.

4. Conclusions

Through a modified HGX-200 continuous-flow cold-vapor generation system, and careful optimization of the instrument gas flow rates, we obtained steady and high signal sensitivity for Hg, and achieved a detection limit of 0.10 ng mL^{-1} for high precision Hg isotope determination. Only 0.70 ng Hg in samples is required using our new method, which enables the direct measurement of low Hg concentration in samples (as low as 5 ng g^{-1}), after direct acid digestion treatment. Using the developed method, the Hg isotopic compositions of four igneous rock SRMs (BCR-2, BHVO-2, GSP-2, and GSR-2) were reported for the first time. The SRMs showed large variations of δ^{202}Hg, indicating that MDF occurred during magmatic processes.

Author contributions

Hongyan Geng and Runsheng Yin contributed equally to this work.

Conflicts of interest

There are no conflicts to declare.

Acknowledgements

This work was supported by the University Research Facility in Chemical and Environmental Analysis (UCEA), The Hong Kong Polytechnic University. Runsheng Yin was funded by the Chinese Academy of Sciences through the Hundred Talent Plan. The rock reference materials were generously provided by Prof. Yuan Honglin (Northwest University, Xi'an, China). This work was financially supported by the Research Grants Council (PolyU 152095/14E), and the National Natural Science Foundation of China (No. 41602047 and 91543205).

References

1 B. A. Bergquist and J. D. Blum, *Elements*, 2009, **5**, 353–357.
2 J. D. Blum, L. S. Sherman and M. W. Johnson, *Annu. Rev. Earth Planet. Sci.*, 2014, **42**, 249–269.
3 R. S. Yin, X. B. Feng, X. D. Li, B. Yu and B. Y. Du, *Trends Environ. Anal. Chem.*, 2014, **2**, 1–10.
4 D. S. Lauretta, B. Klaue, J. D. Blum and P. R. Buseck, *Geochim. Cosmochim. Acta*, 2001, **65**, 2807–2818.
5 D. Foucher and H. Hintelmann, *Anal. Bioanal. Chem.*, 2006, **384**, 1470–1478.
6 J. D. Blum and B. Bergquist, *Anal. Bioanal. Chem.*, 2007, **388**, 353–359.
7 R. B. Georg and K. Newman, *J. Anal. At. Spectrom.*, 2015, **30**, 1935–1944.
8 J. Masbou, D. Point and J. E. Sonke, *J. Anal. At. Spectrom.*, 2013, **28**, 1620–1628.
9 J. E. Sonke, T. Zambardi and J. P. Toutain, *J. Anal. At. Spectrom.*, 2008, **23**, 569–573.
10 X. Fu, L. E. Heimbrger and J. E. Sonke, *J. Anal. At. Spectrom.*, 2014, **29**, 841–852.
11 L. E. Gratz, G. J. Keeler, J. D. Blum and L. S. Sherman, *Environ. Sci. Technol.*, 2010, **44**, 7764–7770.
12 L. S. Sherman, J. D. Blum, G. J. Keeler, J. D. Demers and J. T. Dvonch, *Environ. Sci. Technol.*, 2012, **46**, 382–390.
13 W. Zheng and H. Hintelmann, *J. Phys. Chem. A*, 2010, **114**, 4238–4245.
14 J. D. Demers, J. D. Blum and D. R. Zak, *Global Biogeochem. Cycles*, 2013, **27**, 222–238.
15 J. M. Rolison, W. M. Landing, W. Luke, M. Cohen and V. J. M. Salters, *Chem. Geol.*, 2013, **336**, 37–49.
16 H. Y. Lin, D. X. Yuan, B. Y. Lu, S. Y. Huang, L. M. Sun, F. Zhang and Y. Q. Gao, *J. Anal. At. Spectrom.*, 2015, **30**, 353–359.

17 M. Štrok, H. Hintelmann and B. Dimock, *Anal. Chim. Acta*, 2014, **851**, 57–63.
18 R. S. Yin, D. P. Krabbenhoft, B. A. Bergquist, W. Zheng, R. F. Lepak and J. P. Hurley, *J. Anal. At. Spectrom.*, 2016, **31**, 2060–2068.
19 J. Chen, H. Hintelmann and B. Dimock, *J. Anal. At. Spectrom.*, 2010, **25**, 1402–1409.
20 R. S. Yin, X. B. Feng and J. B. Chen, *Environ. Sci. Technol.*, 2014, **48**, 5565–5574.
21 J. L. Liu, X. B. Feng, R. S. Yin, W. Zhu and Z. G. Li, *Chem. Geol.*, 2011, **287**, 81–89.
22 L. S. Sherman, J. D. Blum, D. K. Nordstrom, R. B. McCleskey, T. Barkay and C. Vetriani, *Earth Planet. Sci. Lett.*, 2009, **279**, 86–96.
23 J. Gray, M. Pribil, P. Van Metre, D. Borrok and A. Thapalia, *Appl. Geochem.*, 2013, **29**, 1–12.
24 R. Y. Sun, M. Enrico, L. E. Heimbürger, C. Scott and J. Sonke, *Anal. Bioanal. Chem.*, 2013, **405**, 6771–6781.
25 C. N. Smith, S. E. Kesler, J. D. Blum and J. J. Rytuba, *Earth Planet. Sci. Lett.*, 2008, **269**, 399–407.